RAPID COMMUNICATIONS

PHYSICAL REVIEW B VOLUME 31, NUMBER 10 15 MAY 1985

Experimental symmetry analysis of energy bands near critical points in Pt using spin- and momentum-resolved photoemission

H. P. Oepen, K. Hünlich, and J. Kirschner
Institut für Grenzflächenforschung und Vakuumphysik, Kernforschungsanlage Jülich, Postfach 1913, D-5170 Jülich, West Germany

A. Eyers, F. Schäfers,* G. Schönhense, and U. Heinzmann
Fritz-Haber-Institut der Max-Planck-Gesellschaft, Faradayweg 6, D-1000 Berlin, West Germany
(Received 4 December 1984)

A theoretical discrepancy concerning band crossings at two points along the Λ direction in Pt is clarified by experimental symmetry analysis of the band characteristics, using circularly polarized synchrotron radiation and spin analysis of the photoelectrons by a new low-energy-diffraction analyzer system. Each of the theoretical results is found to be correct at one k point and incorrect at the other one.

The feasibility of spin- and momentum-resolved photoemission using circularly polarized synchrotron radiation has recently been demonstrated, and its potential for the experimental determination of band-structure symmetries has been pointed out.[1] In the previous experiment,[2] involving a Mott detector, the spin polarization within a photoemission spectrum taken for a number of different photon energies was sampled at a rather limited number of points only. In the experiments reported here, which were done with the low-energy-diffraction spin-polarization detector,[3–5] the polarization distribution over the whole spectrum has been measured at high-point density. This allows the decomposition of the total intensity into two partial intensities of opposite spin polarization, and more subtle features of the band-structure properties become accessible to investigation. In particular, we show how a discrepancy between theoretical band-structure calculations for Pt along Λ can be unequivocally resolved on experimental grounds by harnessing the electron spin polarization.

The discrepancy concerns the qualitative and therefore fundamental question of whether two bands may form a crossing or an anticrossing at a particular point in k space. Figure 1 shows the results of two relativistic band-structure calculations for Pt along Γ–L. Figure 1(b) is due to Mackintosh, published in Ref. 6, representing a non-self-consistent relativistic-augmented-plane-wave (RAPW) calculation. A more elaborate calculation, carried to self-consistency, was published 10 years later by MacDonald, Daams, Vosko, and Koelling,[7] shown in Fig. 1(a). While the two theoretical results are similar in general, they disagree in two important points. Figure 1(a) shows two band crossings at points I and II, while Fig. 1(b) shows two anticrossings at the same points. This striking discrepancy cannot be solved on the basis of published experimental band-mapping data[8] as they are compatible, within the experimental uncertainty, with both theories. Our arguments, however, are based on symmetries rather than energy eigenvalues, and we will show that point I is correctly described in Fig. 1(b), while point II is correct in Fig. 1(a).

The general aspects of the experimental apparatus have been described previously.[2,9] Here we focus on the momentum- and spin-resolving spectrometer system, which is shown schematically in Fig. 2. The uv light from the monochromator (upper half plane for positive helicity, the lower half for negative helicity) passes through the spectrometer system and impinges normally onto the Pt(111) crystal. Normal incidence was chosen in order to avoid changes of the polarization state of the light due to absorption in the metal.[10] Normal takeoff was chosen to suppress final state spin-polarization effects.[11]

Under these conditions the spin-polarization vector is normal to the surface, which was checked experimentally. The above conditions require the electron spectrometer [of the cylindrical-mirror analyzer (CMA) type[4]] to work with a virtual entrance slit located near its symmetry axis. The optical exit slit is identical to the electron-optical entrance aperture at the front end of the electrostatic transport lens. In order to suppress secondary electrons the sample was kept at about -10 V with respect to ground. The angular resolution was estimated to be about $\pm 5°$ on the basis of numerical trajectory calculations.[5] After energy analysis (resolution 0.3–0.4 eV), the electrons are accelerated and focused onto the W(001) crystal. The electrons elastically diffracted from

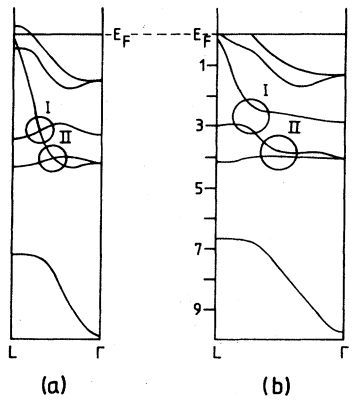

FIG. 1. Theoretical band structures for Pt along the [111] direction as calculated by MacDonald *et al.* (Ref. 7) in (a), and by Mackintosh (published in Ref. 6) in (b). Note the discrepancies at points *A* and *B* where MacDonald *et al.* predict band crossings, whereas Mackintosh finds anticrossings.

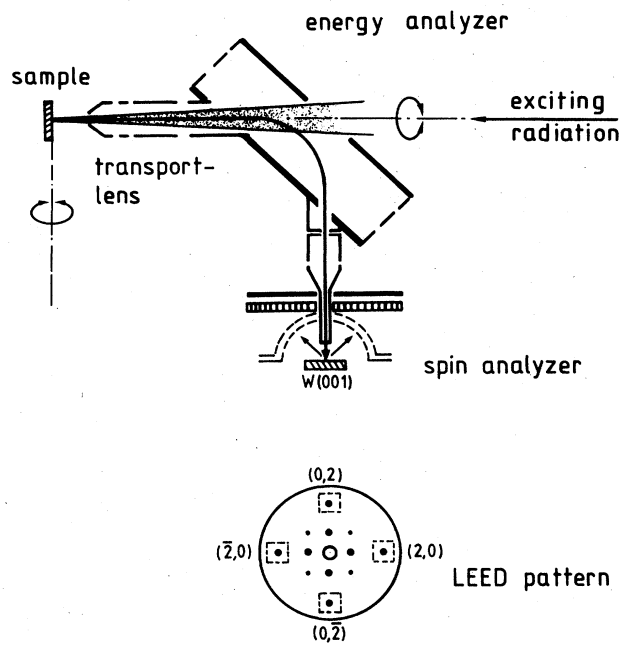

FIG. 2. Schematic view of the spin- and momentum-resolving spectrometer system. The schematic LEED pattern, as obtained on an oscilloscope, indicates the electronic windows and the beams used for polarization analysis.

the W crystal are multiplied by a channel plate and counted by a position-sensitive detector. The low-energy-diffraction (LEED) pattern observed on an oscilloscope screen is shown schematically in the lower part of Fig. 2. Electronic windows are set around the polarization-sensitive ⟨20⟩ beams, and the relative intensity difference of each pair of beams yields one component of the polarization vector. For example, the (02) and (0$\bar{2}$) beams measure the polarization component along the surface normal. The polarization vector can be determined completely by rotating the spectrometer plus spin analyzer about the horizontal axis. Then the (20)-($\bar{2}$0) beam pair measures the polarization vector component normal to the electron momentum and in the paper plane, while the longitudinal component is measured redundantly. Count rates of more than 10^3 sec^{-1} per diffracted beam have been obtained, which allowed measurement of spectra like that in Figs. 3(a) and 3(b) in slightly less than 1 h. During the measurements the vacuum was in the low 10^{-10}-Torr range and the W-detector crystal was flashed in intervals of 15–30 min. This causes an interruption of about 1 min.

Experimental results are shown in Figs. 3 and 4 for positive-helicity light (about 90% circular polarization) of $h\nu = 13$ and 11 eV, respectively. The measured quantities are the total intensity I [Fig. 3(a)] and the polarization P [Fig. 3(b)] as a function of energy below E_F. From these the partial intensities I^+ and I^- may be obtained by means of the relations

$$I^+ = \tfrac{1}{2} I(1+P) \quad \text{and} \quad I^- = \tfrac{1}{2} I(1-P) \ . \tag{1}$$

At each energy these intensities give the number of electrons with spin parallel (I^+) or antiparallel (I^-) to the surface normal. The partial intensities are shown in Fig. 3(c) (denoted by + or −), together with the total intensity I from Fig. 3(a), denoted by dots (statistical error bars omitted). This representation does not contain new information beyond Figs. 3(a) and 3(b), but it considerably aids the interpretation of the spectra. For example, it is clearly seen that the peak A and the shoulder B correspond to peaks in different partial-intensity spectra, as do the features C and D. The final band of nearly free-electron character is the same for all transitions (cf. Fig. 2 in Ref. 2) and is of Λ_6

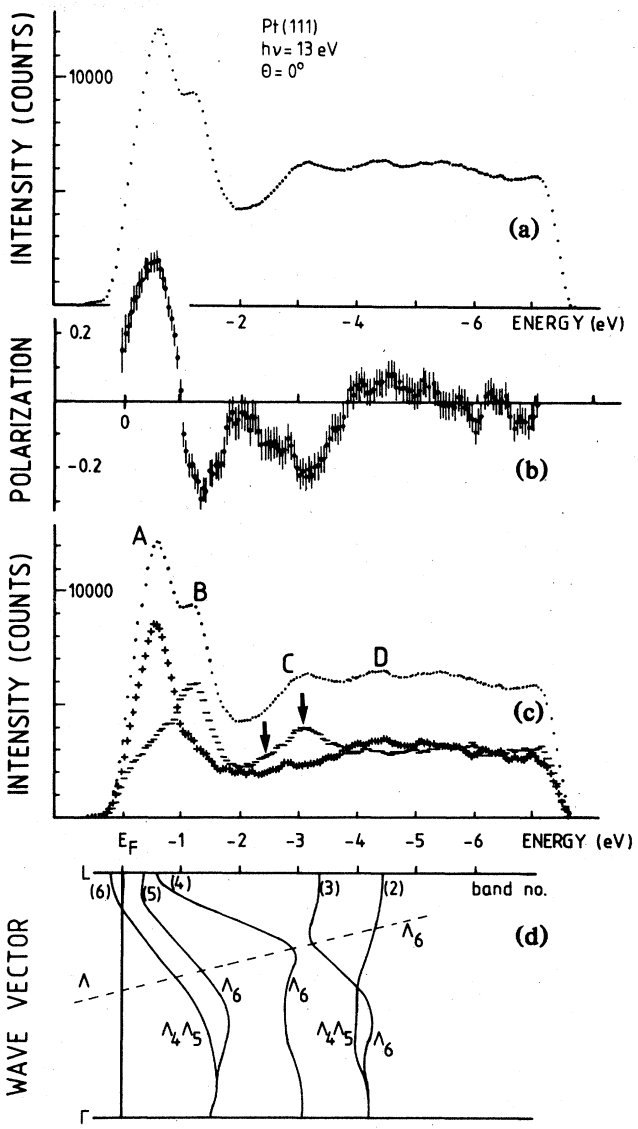

FIG. 3. (a) Total intensity I in the (02)-(0$\bar{2}$) beam pair as a function of binding energy at $h\nu = 13$ eV for normal takeoff. (b) Spin polarization as a function of binding energy. The error bars correspond to the variance of the Poisson distribution. (c) Total intensity I and partial intensities I^+ (+) and I^- (−). Features A–D are discussed in the text. (d) Theoretical band structure of Pt along Λ, with symmetry labels as determined from the spin-polarization analysis. The bands are numbered at the L point with increasing energy [band (1) is off scale] (after Ref. 2). The dashed line corresponds to the final-state band, shifted by 13 eV.

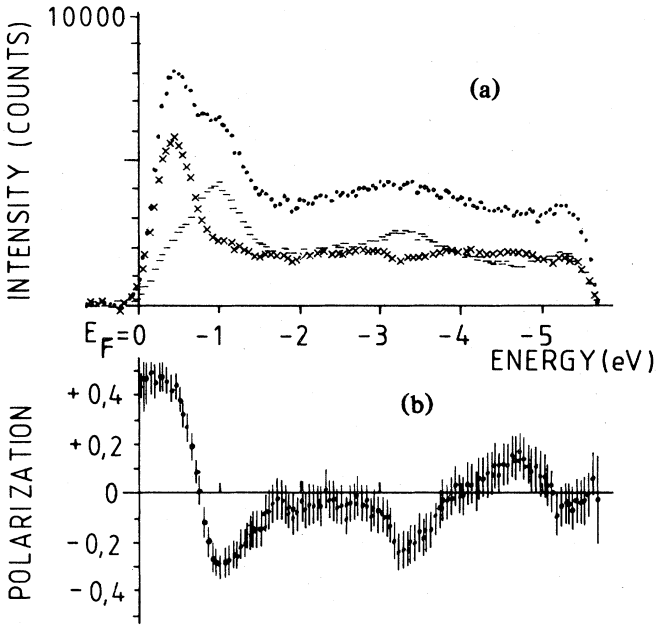

FIG. 4. (a) Total intensity I and partial intensities I^+ (×), I^- (−) at $h\nu = 11$ eV as a function of binding energy. (b) Spin polarization as a function of energy. The positive and negative extrema correspond to emission from bands (6) (close to E_F), (5), (3), and (2) in Fig. 3(d).

symmetry. A parabola has been fitted to it, which is shown in Fig. 3(d) shifted by $h\nu = 13$ eV, together with a theoretical band structure due to Borstel.[2] As peaks B and C appear in the same partial-intensity curve, it follows that the initial states must be of the same symmetry type (Λ_6 in this case), while peaks A and D both belong to states of $\Lambda_4\Lambda_5$ symmetry (time-reversal degenerate). While in the total intensity curve the feature C appears as a single broad peak, the polarization curve and, even more clearly, the partial intensity curve I^- reveal structures near −2.5 eV that have to be attributed to a second peak of minor intensity [marked by arrows in Fig. 3(c)]. A look at Fig. 3(d) shows that these transitions occur near the critical point I of Figs. 1(a) and 1(b). *As the sign of both peaks is the same, the initial states must be of the same symmetry. Hence, the two bands in question cannot cross but must form an anticrossing.* As this statement relies on symmetry properties only, it holds irrespective of quantitative details such as the precise amount of splitting, the precise knowledge of the final-state band, the precise location in k space, or the quantitative agreement between measured and calculated energy eigenvalues.

Further results are shown in Fig. 4 for $h\nu = 11$ eV. The transitions occur closer to the L point in this case, but into the same final band. The first two peaks, corresponding to the spin-orbit-split bands 6 and 5 in Fig. 3(d), are identified as before. A broad hump in the total intensity between −2 and −4 eV contains a transition from a Λ_6-type band, as is clearly seen in the polarization and partial-intensity curves. This corresponds to a transition from band 3. Corresponding results have been found on the other side of the critical point I at $h\nu = 15$ eV. Then band 4 yields a well-defined peak of negative polarization, while band 3 comes only weakly. The transition from band 2 can also be identified in Fig. 4 from the positive polarization at about −4.5 eV, while it is hardly discernible in the total intensity. Because of the sign of the spin polarization, band 2 must be of $\Lambda_4\Lambda_5$ symmetry, while band 3 is of Λ_6 symmetry. Thus, the two bands are of unlike symmetry and a band crossing is allowed. Our band-mapping data for band 2 agree quite well with those of Ref. 8, where also band 3 is visible (which is weak in our case because of s-polarized light). The region II in Fig. 1 is thus characterized by a band crossing [in agreement with Fig. 1(a)], while region I is characterized by an anticrossing [in agreement with Fig. 1(b)]. These features are correctly found in the band structure of Fig. 3(d). This band structure, based on a non-self-consistent RAPW calculation, agrees closely with a recent self-consistent calculation in Ref. 12. The magnitude of the spin-orbit gap, however, is smaller in both calculations (~ 300 meV) than in the previous calculation of Ref. 6 (600–650 meV). The experimental value as determined from the spin-resolved data is approximately halfway between both (~ 500 meV).

In summary, spin- and momentum-resolved photoemission using circularly polarized light allows us to determine not only energy eigenvalues in k space, but also the symmetry properties of the corresponding wave functions. The behavior of bands near critical points (crossings or anticrossings) can be judged from their symmetries alone. The experimental determination of symmetries by spin-polarization analysis thus is expected to open a new field in photoemission.

*Present address: Berliner Elektronenspeicherring-Gesellschaft für Synchrotronstrahlung m.b.H., Lentzeallee 100, D-1000 Berlin 33, West Germany.

[1]H. P. Oepen, A. Eyers, U. Heinzmann, N. Müller, F. Schäfers, G. Schönhense, and J. Kirschner, in Proceedings of the Ninth International Vacuum Congress and Fifth International Conference on Solid Surfaces, Sept. 26–30, 1983, Madrid, Spain (unpublished), extended abstract SSP 9D, p. 76; A. Eyers, J. Kirschner, N. Müller, H. P. Oepen, F. Schäfers, G. Schönhense, and U. Heinzmann, Ann. Isr. Phys. Soc. **6**, 354 (1983).

[2]A. Eyers, F. Schäfers, G. Schönhense, U. Heinzmann, H. P. Oepen, K. Hünlich, J. Kirschner, and G. Borstel, Phys. Rev. Lett. **52**, 1559 (1984).

[3]J. Kirschner and R. Feder, Phys. Rev. Lett. **42**, 1008 (1979).

[4]H. P. Oepen, Ph.D. thesis, Rheinische-Westfälische Technische Hochschule, Aachen, Germany, 1984 (unpublished).

[5]K. Hünlich, Diploma thesis, Rheinische-Westfälische Technische Hochschule, Aachen, Germany, 1984 (unpublished).

[6]O. K. Andersen, Phys. Rev. B **2**, 883 (1970).

[7]A. H. MacDonald, J. M. Daams, S. H. Vosko, and D. D. Koelling, Phys. Rev. B **23**, 6377 (1981).

[8]K. A. Mills, R. F. Davis, S. D. Kevan, G. Thornton, and D. A. Shirley, Phys. Rev. B **22**, 581 (1980).

[9]A. Eyers, Ch. Heckenkamp, F. Schäfers, G. Schönhense, and U. Heinzmann, Nucl. Instrum. Methods **208**, 303 (1983).

[10]P. J. Feibelman, Phys. Rev. B **14**, 762 (1976).

[11]J. Kirschner, R. Feder, and J. F. Wendelken, Phys. Rev. Lett. **47**, 614 (1981).

[12]G. Leschik, R. Courths, H. Wern, S. Hüfner, H. Eckardt, and J. Noffke, Solid State Commun. **52**, 221 (1984).